

# *LISA* detection of massive black hole binaries: imprint of seed populations and of extreme recoils

A Sesana<sup>1</sup>, M Volonteri<sup>2</sup> and F Haardt<sup>3</sup>

<sup>1</sup> Center for Gravitational Wave Physics at the Pennsylvania State University,  
University park, State College, PA 16802, USA

<sup>2</sup> Department of Astronomy, University of Michigan, 500 Church Street, Ann  
Arbor, MI 48109, USA

<sup>3</sup> Dipartimento di Fisica e Matematica, Università dell'Insubria, via Valleggio  
11, 22100 Como, Italy

**Abstract.** All the physical processes involved in the formation, merging, and accretion history of massive black holes along the hierarchical build-up of cosmic structures are likely to leave an imprint on the gravitational waves detectable by future space-borne missions, such as *LISA*. We report here the results of recent studies, carried out by means of dedicated simulations of black hole build-up, aiming at understanding the impact on *LISA* observations of two ingredients that are crucial in every massive black hole formation scenario, namely: (i) the nature and abundance of the first black hole seeds and (ii) the large gravitational recoils following the merger of highly spinning black holes. We predict *LISA* detection rates spanning two order of magnitude, in the range 3-300 events per year, depending on the detail of the assumed massive black hole seed model. On the other hand, large recoil velocities do not dramatically compromise the efficiency of *LISA* observations. The number of detections may drop substantially (by  $\sim 60\%$ ), in scenarios characterized by abundant light seeds, but if seeds are already massive and/or relatively rare, the detection rate is basically unaffected.

## 1. Introduction

Massive black hole (MBH) binaries (MBHBs) are among the primary candidate sources of gravitational waves (GWs) at mHz frequencies [1, 2, 3, 4, 5], the range probed by the space-based *Laser Interferometer Space Antenna* (*LISA*, [6]). Today, MBHBs are ubiquitous in the nuclei of nearby galaxies [7]. If MBHBs were also common in the past (as implied by the notion that many distant galaxies harbor active nuclei for a short period of their life), and if their host galaxies experience multiple mergers during their lifetime, as dictated by popular cold dark matter (CDM) hierarchical cosmologies, then MBHBs inevitably formed in large numbers during cosmic history. MBHBs that are able to coalesce in less than a then Hubble time give origin to the loudest GW signals in the Universe. Provided MBHBs do not “stall”, their GW driven inspiral will then follow the merger of galaxies and protogalactic structures at high redshifts. A low-frequency detector like *LISA* will be sensitive to GWs from coalescing binaries with total masses in the range  $10^3 - 10^6 M_\odot$  out to  $z \sim 10 - 15$  [8].

The formation and evolution of MBHBs has been investigated recently by several groups in the framework of hierarchical clustering cosmology [9, 10, 11]. *LISA* detection rate, ranging from a few to a few hundred per year, were derived in a

number of papers [3, 4, 5, 12]. A comprehensive understanding of the details of MBH formation and evolution are essential in assessing *LISA* detection efficiency and in planning sensible data analysis strategies.

In two recent papers [13, 14], we considered in detail two important ingredients of the MBH formation route. (i) *The nature and abundance of the first black hole seeds*. Our understanding of seed black hole formation is extremely poor. There are several proposed formation mechanisms resulting in a broad spectrum of possible seed populations [15, 11, 16, 17]. Following [13], we investigate different physically and cosmologically motivated seed formation routes, showing their imprint on the expected MBHB coalescence rate and hence on *LISA* detection. (ii) *Extreme gravitational recoils*. Recent relativistic numerical simulations of merging spinning black hole binaries have shown that the remnant may get a kick of the order of a few thousand km/s [18, 19], which is likely to eject it even from the center of a giant elliptical (escape velocity  $\gtrsim 2000$  km/s), with important astrophysical implications [20, 21, 22]. We incorporate the effect of extreme gravitational recoils following the merger of highly spinning black holes in our hierarchical models [14], exploring its consequences on the GW detection side.

We highlight in this paper the main results reported in [13, 14], focusing on their implications for *LISA* detections and assessing *LISA* capability to place constraints on MBH formation scenarios, looking for reliable diagnostics to discriminate between the different models. The plan of the paper is as follow. In Section 2, we describe the general framework of MBHB formation in hierarchical scenarios. We briefly discuss the issue of GW detection with *LISA* in Section 3, and then in Section 4 and 5 we discuss the impact of the seed black hole population and of the gravitational recoil prescription on *LISA* observations. We summarize our findings in Section 6.

## 2. Hierarchical models of black hole formation

In the hierarchical framework of structure formation [23, 24], MBHs grow starting from pregalactic seed black holes formed at early times. MBH evolution then follows the merging history of their host galaxies and dark matter halos. The merger process would inevitably form a large number of MBHBs during cosmic history. In our models we apply the extended Press & Schechter EPS formalism [25, 26, 27] to the hierarchical assembly of dark matter halos, using a range of prescriptions for the evolution of the population of MBHs residing in the halo centers. The halo hierarchy is followed by means of Monte Carlo realizations of the merger hierarchy. Each model is constructed tracing backwards the merger hierarchy of 220 dark matter halos in the mass range  $10^{11} - 10^{15} M_{\odot}$  up to  $z = 20$  [10], then populating the halos with seed black holes and following their evolution to the present time. Nuclear activity is triggered by halo mergers: in each major merger the more massive hole accretes gas until its mass scales with the fifth power of the circular velocity of the host halo, normalized to reproduce the observed local correlation between MBH mass and velocity dispersion ( $m_{\text{BH}} - \sigma_*$  relation [28]). Gas accretion onto the MBHs is assumed to occur at a fraction of the Eddington rate. In the boundaries given by this general framework, there is a certain freedom in the choice of the seed masses, in the accretion prescription, and in the MBHB coalescence efficiency.

### 2.1. MBHB dynamics

During a galactic merger, the central MBHs initially share their fate with the host galaxy. The merging is driven by dynamical friction, which has been shown to efficiently merge the galaxies and drive the MBHs in the central regions of the newly formed galaxy when the mass ratio of the satellite halo to the main halo is sufficiently large [29]. The efficiency of dynamical friction decays when the MBHs get close and form a binary. In gas-poor systems, the subsequent evolution of the binary may be largely determined by three-body interactions with background stars [30], leading to a long coalescence timescale. In gas rich high redshift halos, the orbital evolution of the central MBH is likely dominated by dynamical friction against the surrounding gaseous medium. The available simulations [31, 32] show that the binary may shrink to about parsec or slightly subparsec scale by dynamical friction against the gas, depending on the gas thermodynamics. We have assumed here that, if a hard MBH binary is surrounded by an accretion disc, it coalesces instantaneously owing to interaction with the gas disc. If instead there is no gas readily available, the binary will be losing orbital energy to the stars, using the scheme described in [10].

Assuming efficient coalescence for the MBH pairs, for each of the 220 halos all the coalescence events happening during the cosmic history are collected. The outputs are then weighted using the EPS halo mass function and integrated over the observable volume shell at every redshift to obtain numerically the coalescence rate of MBHBs as a function of black hole masses and redshift.

## 3. Gravitational wave signal

Full discussion of the GW signal produced by an inspiraling MBHB can be found in [5], along with all the relevant references. Here we just recall that a MBHB at (comoving) distance  $r(z)$  with chirp mass  $\mathcal{M} = m_1^{3/5} m_2^{3/5} / (m_1 + m_2)^{1/5}$  ( $m_1 > m_2$  are the two MBH masses) generates a GW signal with a characteristic strain given by:

$$h_c = \frac{1}{3^{1/2} \pi^{2/3}} \frac{G^{5/6} \mathcal{M}^{5/6}}{c^{3/2} r(z)} f_r^{-1/6}, \quad (1)$$

where  $G$  and  $c$  have their standard meaning. An inspiraling binary is then detected if the signal-to-noise ratio ( $S/N$ ) *integrated over the observation* is larger than a given detection threshold, where the optimal  $S/N$  is given by [33]

$$S/N = \sqrt{\int d \ln f \left[ \frac{h_c(f_r)}{h_{\text{rms}}(f)} \right]^2}. \quad (2)$$

Here,  $f = f_r / (1 + z)$  is the (observed) frequency emitted at time  $t = 0$  of the observation, and the integral is performed over the frequency interval spanned by the shifting binary during the observational time. Finally,  $h_{\text{rms}} = \sqrt{5f S_h(f)}$  is the effective rms noise of the instrument;  $S_h(f)$  is the one-sided noise spectral density, and the factor  $\sqrt{5}$  takes into account for the random directions and orientation of the wave;  $h_{\text{rms}}$  is obtained by adding in the instrumental noise contribution (given by e.g. the Larson's online sensitivity curve generator <http://www.srl.caltech.edu/~shane/sensitivity>), and the confusion noise from unresolved galactic [34] and extragalactic [35] WD–WD binaries. Notice that extreme mass-ratio inspirals (EMRIs) could also contribute to the confusion noise in the mHz frequency range [36]. All the results shown in the following sections assume

a *LISA* operation time of 3 years, a cut-off at  $10^{-4}$  Hz in the instrumental sensitivity and a detection integrated threshold of  $S/N = 5$  (equation 2).

#### 4. Seed black hole population imprint

In this section we investigate the influence of different seed population prescriptions on *LISA* detections. In all the models described below, we assume non spinning binaries; the coalescence remnant thus experiences only a mild recoil, that is never larger than  $\sim 250$  km/s [37, 38]. The effects of extreme gravitational recoil associated to the coalescence of highly spinning MBHs will be separately explored in Section 5.

##### 4.1. Description of the models

Several scenarios has been proposed for the seed black hole formation: seeds of  $m_{\text{seed}} \sim \text{few} \times 100 M_{\odot}$  can form as remnants of metal free (PopIII) stars at redshift  $\gtrsim 20$  (as assumed by Volonteri, Haardt and Madau [10], hereinafter VHM model), while intermediate-mass seeds ( $m_{\text{seed}} \sim 10^5 M_{\odot}$ ) can be the endproduct of the dynamical instabilities arising in massive gaseous protogalactic disks in the redshift range  $10 \lesssim z \lesssim 15$  (as investigated by Koushiappas, Bullock and Dekel [11], hereinafter KBD model; or by Begelman, Volonteri and Rees [16], hereinafter BVR model).

In the VHM model, pregalactic seed holes form with intermediate masses ( $m_{\text{seed}} \sim 150 M_{\odot}$ ) as remnants of the first generation of massive metal-free stars with  $m_* > 260 M_{\odot}$  that do not disappear as pair-instability supernovae [15]. We place them in isolation within halos above  $M_H = 1.6 \times 10^7 M_{\odot}$  collapsing at  $z = 20$  from rare  $> 3.5\sigma$  peaks of the primordial density field. While  $Z = 0$  stars with  $40 < m_* < 140 M_{\odot}$  are also predicted to collapse to MBHs with masses exceeding half of the initial stellar mass [39], the merger rate of MBHBs in the mass range relevant to *LISA* observations is not very sensitive to the precise choice for the seed hole mass.

A different class of models assumes that MBH seeds form already massive. In the KBD model, seed MBHs form from the low angular momentum tail of material in halos with efficient molecular hydrogen gas cooling. MBHs with mass

$$m_{\text{seed}} \simeq 5 \times 10^4 M_{\odot} (M_H / 10^7 M_{\odot}) (1 + z/18)^{3/2} (\lambda / 0.04)^{3/2} \quad (3)$$

form in in dark matter halos with mass

$$M_H \gtrsim 10^7 M_{\odot} (1 + z/18)^{-3/2} (\lambda / 0.04)^{-3/2}. \quad (4)$$

We have fixed the free parameters in equation 3 by requiring an acceptable match with the luminosity function of quasars at  $z < 6$ . Here  $\lambda$  is the so called spin parameter, which is a measure of the angular momentum of a dark matter halo  $\lambda \equiv J|E|^{1/2}/GM_H^{5/2}$ , where  $J$ ,  $E$  and  $M_H$  are the total angular momentum, energy and mass of the halo. The angular momentum of galaxies is believed to have been acquired by tidal torques due to interactions with neighboring halos. The distribution of spin parameters found in numerical simulations is well fit by a lognormal distribution in  $\lambda_{\text{spin}}$ , with mean  $\bar{\lambda}_{\text{spin}} = 0.04$  and standard deviation  $\sigma_{\lambda} = 0.5$  [40, 41]. We have assumed that the MBH formation process proceeds until  $z \approx 15$ .

In the BVR model, black hole seeds form in halos subject to runaway gravitational instabilities, via the so called "bars within bars" mechanism [42]. We assumed here,

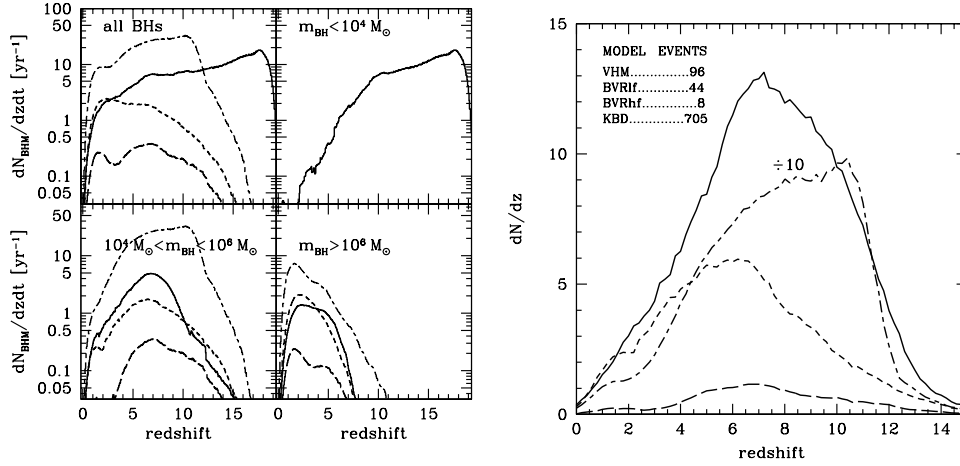


**Figure 1.** *Left panel:* number of MBHB coalescences per observed year at  $z = 0$ , per unit redshift, in different  $m_{\text{BH}} = m_1 + m_2$  mass intervals. *Solid lines:* VHM model; *short-long dashed lines:* KBD model; *short-dashed lines:* BVRlf model; *long-dashed lines:* BVRhf model. *Right panel:* redshift distribution of MBHBs resolved with  $S/N > 5$  by LISA in a 3-year mission. Line style as in the left panel. The number of events predicted by KBD model (*long-short dashed curve*) is divided by a factor of 10. The top-left corner label lists the total number of expected detections.

as in BVR, that runaway instabilities are efficient only in metal free halos with virial temperatures  $T_{\text{vir}} \gtrsim 10^4 \text{K}$ . The “bars within bars” process produces in the center of the halo a “quasistar” (QSS) with a very low specific entropy. When the QSS core collapses, it leads to a seed black hole of a few tens solar masses. Accretion from the QSS envelope surrounding the collapsed core can however build up a substantial black hole mass very rapidly until it reaches a mass of the order the “quasistar” itself,  $m_{\text{QSS}} \simeq 10^4 - 10^5 M_\odot$ . The seed black hole accretion rate adjusts so that the feedback energy flux equals the Eddington limit for the quasistar mass; thus, the black hole grows at a super-Eddington rate as long as  $m_{\text{QSS}} > m_{\text{seed}}$ . The result is that  $m_{\text{seed}}(t) \sim 4 \times 10^5 (t/10^7 \text{ yr})^2 M_\odot$  i.e.,  $m_{\text{seed}} \propto t^2$ . In metal rich halos star formation becomes efficient, and depletes the gas inflow before the conditions for QSS (and MBH) formation are reached. BVR envisage that the process of MBH formation stops when gas is sufficiently metal enriched. We consider here two scenarios, one in which star formation exerts a high level of feedback and ensures a rapid metal enrichment (BVRhf), one in which feedback is milder and halos remain metal free for longer (BVRlf). In the former case MBH formation ceases at  $z \approx 18$ , in the latter at  $z \approx 15$ . The BVRhf model appears to produce barely enough MBHBs to reproduce the observational constraints (ubiquity of MBHBs in the local Universe, luminosity function of quasars). We consider it a very strong lower limit to the number of seeds that need to be formed in order to fit the observational constraints.

#### 4.2. Coalescence rates and LISA detections

Different seed populations would inevitably leave a peculiar imprint on the merger rate of MBHBs relevant to LISA. Left panel of figure 1 shows the number of MBH

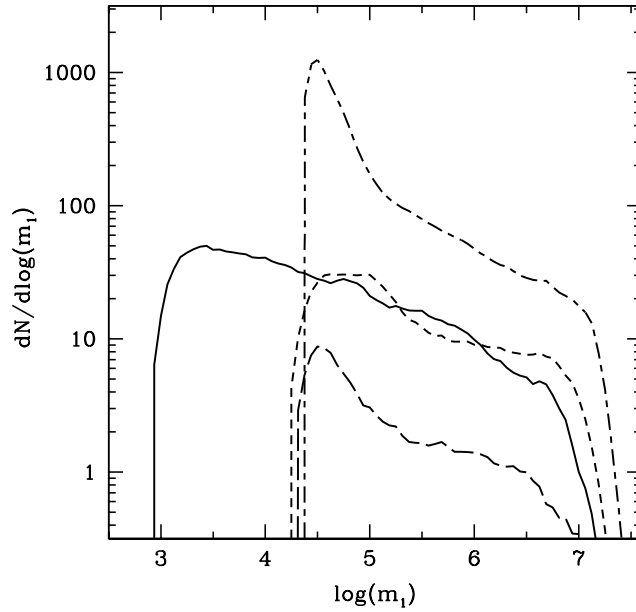


**Figure 2.** Mass function of the more massive member of MBHBs resolved with  $S/N > 5$  by *LISA* in a 3-year mission. Line style as in figure 1. All curves are normalized such as the integral in  $d\log(m_1)$  gives the number of detected events.

binary coalescences per unit redshift per unit *observed* year,  $dN/dzdt$ , predicted by the five models we tested. Each panel shows the rates for different  $m_{\text{BH}} = m_1 + m_2$  mass intervals. The total coalescence rate spans almost two orders of magnitude ranging from  $\sim 3 \text{ yr}^{-1}$  (BVRhf) to  $\sim 250 \text{ yr}^{-1}$  (KBD). As a general trend, coalescences of more massive MBHBs peak at lower redshifts (for all the models the coalescence peak in the case  $m_{\text{BH}} > 10^6 M_\odot$  is at  $z \sim 2$ ). Note that there are no merging MBHBs with  $m_{\text{BH}} < 10^4 M_\odot$  in the KBD and BVR models.

Right panel of figure 1 shows the redshift distribution of *LISA* MBHB detections. The KBD model results in a number of events ( $\simeq 700$ ) that is more than an order of magnitude higher than that predicted by other models, with a skewed distribution peaked at sensibly high redshift,  $z \gtrsim 10$ . It is interesting to compare the *number of detections* with the *total number of binary coalescences* predicted by the different formation models. The KBD model produces  $\simeq 750$  coalescences, the VHM model  $\simeq 250$ , and the two BVR models just few tens. A difference of a factor  $\simeq 3$  between the KBD and the VHM models in the total number of coalescences, results in a difference of a factor of  $\simeq 10$  in the *LISA* detections, due to the different mass of the seed black holes. Almost all the KBD coalescences involve massive binaries ( $m_1 \gtrsim 10^4 M_\odot$ ), which are observable by *LISA*. The KBD and BVR models differ for the sheer number of MBHBs. The halo mass threshold in the KBD model is well below (about 3 orders of magnitude) the BVR one, the latter requiring halos with virial temperature above  $10^4 \text{ K}$ . In a broader context, results pertaining to the KBD model describe the behavior of families of models where efficient MBH formation can happen also in mini-halos where the source of cooling is molecular hydrogen.

It is difficult, on the basis of the redshift distributions of detected binaries only, to discriminate between heavy and light MBH seed scenarios. Although the VHM and BVRlf models predict a different number of observable sources, the uncertainties in the models are so high, that a difference of a factor of two (96 for the VHM model, 44 for the BVRlf model) cannot be considered a safe discriminant. Moreover the redshift distributions are quite similar, peaked at  $z \simeq 6 - 7$  and without any particular feature in the shape. In [5] we showed that *LISA* will be sensitive to binaries with masses  $\lesssim 10^3 M_\odot$  up to redshift ten. Hence the discrimination between heavy and light MBH seed scenarios should be easy on the basis of the mass function of detected binaries. This is shown in figure 2. As expected, in the VHM model, the mass distribution extends to masses  $\lesssim 10^3 M_\odot$ , giving a clear and unambiguous signature of a light seed scenario. VHM predict that many detections (about 50%) involve low mass binaries ( $m_{\text{BH}} < 10^4 M_\odot$ ) at high redshift ( $z > 8$ ). These sources are observable during the inspiral phase, but their frequency at the last stable orbit  $f_{\text{LSO}}$  is too high for *LISA* detection (see [5], figure 2). Heavy seed scenarios predict instead that the GW emission at  $f_{\text{LSO}}$ , and the subsequent plunge are always observable for all binaries.

## 5. Gravitational recoil imprint

In all the models detailed in the previous section, we implemented a ‘conservative’ recoil prescription appropriate to mergers of non spinning black holes. In the following, we quantify, for selected seed scenarios, the maximum effect that gravitational recoil may have on *LISA* detection rates.

### 5.1. Description of the models

We focus here on two specific models described in Section 4.1, that are representative of these two classes of MBH seed formation scenarios: the VHM and the BVRlf models. For both of them, we consider two cases that bound the effect of recoil in the assembly of MBHs and, as a consequence, *LISA* events: (i) no gravitational recoil takes place and (ii) maximal gravitational recoil is associated to every MBHB merger, using the model by Volonteri 2007 [22], which is based on the estimates reported by Campanelli et al. 2007 [19]. For the latter we use the merger tree realizations presented in [22]. The model takes into account consistently for the cosmic evolution of the mass ratio distribution of merging binaries and of their spin parameters (see discussion in [22]). The spin orientations during each merger are instead always in the configuration leading to the maximum recoil according to [19], i.e., MBH spins are assumed to lie in the binary orbital plane counter-aligned one to each other. The recoil velocity is then computed according to equation 1 of [19] assuming  $\Theta = \Theta_0$  (i.e., the maximum possible recoil velocity). We would like to emphasize that the prescription that we have chosen for (ii), and whose main features we have just summarized is the least favorable for GW observations and (probably) unlikely to occur in these extreme circumstances during MBH assembly.

### 5.2. Merger rates and *LISA* detections

Left panel of figure 3 shows the number of MBH binary coalescences per unit  $\log \mathcal{M}$  per unit *observed* year,  $dN/d\log \mathcal{M} dt$ , predicted by the two models that we have considered, for both cases where recoil is neglected and extreme recoil is taken into account. Each

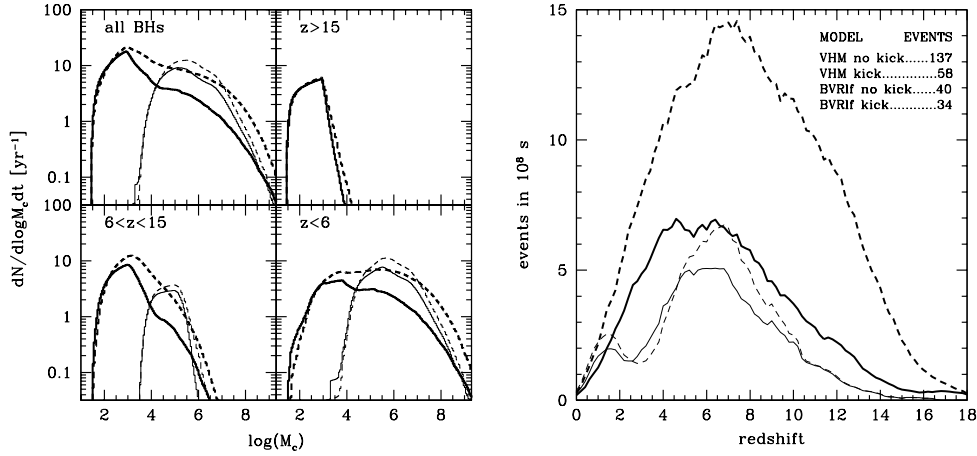


**Figure 3.** *Left panel:* number of MBHB coalescences per observed year at  $z = 0$ , per unit log chirp mass, in different redshift intervals. *Dashed lines:* GW recoil neglected; *solid lines:* extreme GW recoil included. *Thick lines:* VHM model; *thin lines:* BVRlf model. *Right panel:* redshift distribution of MBHBs resolved with  $S/N > 5$  by *LISA* in a 3-year mission. Line style as in the left panel. The top-right corner label lists the total number of expected detections.

panel shows the rates for different redshift intervals. Note that when extreme recoil is included, the rate predicted by the BVRlf model at any redshift is only marginally affected, while the VHM model is more sensitive to the GW recoil: at  $z > 15$ , GW kicks do not affect the coalescence rate; on the contrary, at  $z < 15$ , the rate drops by a factor of  $\sim 3$  for  $M \gtrsim 10^3 M_\odot$ , if extreme kicks are included in the evolution. This is related to the fraction of seeds that experience multiple coalescences during the MBH assembly history. We can schematically think of the assembly history as a sequence of coalescence rounds. After each round extreme recoil depletes a large fraction of remnants, and the relative importance of each subsequent round drops accordingly. In the VHM model, about 65% of the remnants of the first round will undergo a second round of coalescences, so the second round has an important relative weight in the computation of the total rate. When extreme recoil is taken into account, a large fraction of the first round remnants is ejected from their hosting halos. We find that the effective fraction of remnants that can experience a second coalescence drops to  $\sim 30\%$ . This is the reason why the number of coalescences involving light black holes ( $M < 10^3 M_\odot$ ) does not drop at any redshift, while the number of coalescences involving more massive binaries drops by a factor  $\approx 3$ . In the BVRlf scenario seeds are rarer, and the fraction of first coalescence remnants that participate to the second round is around 25%; switching on the extreme recoil has a significantly smaller impact on the global rate in this case. Moreover, in this model seeds are more massive and the bulk of merging events happens at lower redshift, where the hosting halo potential wells are deeper and consequently larger kicks are needed to eject the coalescence remnants. As a matter of fact, the seed abundance sets the mean number of major mergers that a seed is expected to undergo during the cosmic history, and this basically sets the ability of extreme kicks to reduce the coalescence rate.

Right panel of figure 3 shows the redshift distribution of MBHBs detected by



*LISA*. The effect of extreme GW recoils on the source number counts drastically depends on the abundance and nature of the seeds. In the VHM model, the number of detectable sources drops by a factor  $\sim 60\%$ , and the number of the potential *LISA* detections is reduced from  $\approx 140$ , if the recoil is neglected, to  $\approx 60$ , if extreme recoil is included. Vice versa, the detection rate predicted by the BVRlf model is only weakly affected by the extreme recoil prescription, and it drops by about 15% (from 40 to 34 events in 3 years of observation  $\ddagger$ ). Note that though the overall number of coalescences in the VHM model decreases only by about 25% when extreme recoil is considered, the number of *LISA* detections is reduced by a much larger factor. This is because if the seeds are light, *LISA* can not detect the bulk of the first coalescences of light binaries happening at high redshift, that are responsible for the major contribution to the coalescence rate and are not affected by the recoil. *LISA* can observe later events, involving more massive binaries, that are largely suppressed by the MBH depopulation due to extreme GW kicks. In the BVRlf model, on the other hand, seeds are more massive, and the second coalescence round is less important; in this case, the *LISA* sensitivity is sufficient to observe almost all the first coalescences, and the number of detections is only mildly reduced.

## 6. Summary and conclusions

Using dedicated Monte Carlo simulations of the hierarchical assembly of dark matter halos along the cosmic history, we have computed the expected gravitational wave signal from the evolving population of massive black hole binaries. We investigated the imprint of different seed black hole formation routes and on extreme recoils on *LISA* detections.

We found that a large fraction (depending on models) of coalescences will be directly observable by *LISA*, and on the basis of the detection rate, constraints can be put on the MBH formation process. Detection of several hundreds events in 3 years will be the sign of a efficient formation of heavy MBH seeds in a large fraction of high redshift halos (KBD). On the other extreme, a low event rate, about few tens in 3 years, is peculiar of scenarios where either the seeds are light, and many coalescences do not fall into the *LISA* band, or seeds are massive, but rare, as envisioned by, e.g., BVR (see also [17]). In this case a decisive diagnostic is provided by the mass distribution of detected events. In the light seed scenario, the mass distribution of observed binaries extend to  $\sim 10^3 M_\odot$ , while there are no sources with mass below  $10^4 M_\odot$  in the high seed scenario.

We have then considered two specific MBH assembly models (VHM, BVRlf), representative of two different MBH seed formation scenarios. For both of them, we investigated two cases that bound the effect of recoil in the assembly of MBHs and, as a consequence, *LISA* events: (i) no gravitational recoil takes place and (ii) maximal gravitational recoil is associated to every MBHB merger, using the model described in [22]. Our results show that at time it is not clear if *LISA* will be able to shed light on the importance of recoil in MBH assembly, even in this extreme case, since the uncertainty introduced in the number counts is at most of a factor of  $\sim 3$ , comparable

$\ddagger$  Note that both numbers are smaller than 44, which is the numbers of event found in Section 4 assuming a non-spinning recoil prescription. This is consistent with a Poissonian variance in the number of coalescences for different Monte Carlo realizations of the seed populations. The 15% decrease found here (from 40 to 34) is instead computed starting from the same Monte Carlo realization of the seed population, and then applying different recoil recipes.

with uncertainties due to our ignorance in the MBH accretion history and in the detailed dynamics of MBHBs (see, e.g., discussion in [13]). On the other hand, this fact confirm that MBHBs are *LISA* safe targets; since extreme recoil effects increase with the seed abundance, we expect the drop in the detections to be more significant for those scenarios that predict a larger number of sources.

In conclusions, from the point of detection of low frequency gravitational waves, massive black hole binaries are certainly one of the major target for the *LISA* mission, independently on the actual seed black hole formation route and on the magnitude of the typical recoil suffered by the remnants of binary coalecences. On the astrophysical ground, *LISA* will be a unique probe of the formation, accretion and merger of MBHs along the *entire* cosmic history of galactic structures.

## References

- [1] Haehnelt M. G., 1994, MNRAS, 269, 199
- [2] Jaffe A. H. & Backer D. C., 2003, ApJ, 583, 616
- [3] Wyithe J. S. B. & Loeb A., 2003, ApJ, 590, 691
- [4] Sesana A., Haardt F., Madau P. & Volonteri M., 2004, ApJ, 611, 623
- [5] Sesana A., Haardt F., Madau P. & Volonteri M., 2005, ApJ, 623, 23
- [6] Bender P. L. et al., 1998 *LISA Pre-Phase A Report; Second Edition*, MPQ 233
- [7] Magorrian J. et al., 1998, AJ, 115, 2285
- [8] Hughes S. A., 2002, MNRAS, 331, 805
- [9] Menou K., Haiman Z. & Narayanan V. K., 2001, ApJ, 558, 535
- [10] Volonteri M., Haardt F. & Madau P., 2003, ApJ, 582, 599
- [11] Koushiappas S. M., Bullock J. S. & Dekel A., 2004, MNRAS, 354, 292
- [12] Rhook K. J. & Wyithe J. S. B., 2005, MNRAS, 361, 1145
- [13] Sesana A., Volonteri M. & Haardt F., 2007, MNRAS, 377, 1711
- [14] Sesana A., 2007, MNRAS, 382, 6
- [15] Madau P. & Rees M. J., 2001, ApJ, 551, L27
- [16] Begelman M. C., Volonteri & Rees M. J., 2006, MNRAS, 370, 289
- [17] Lodato G. & Natarajan P., 2006, MNRAS, 371, 1813
- [18] Tichy W. & Marronetti P., 2007, PhRvD, 061502
- [19] Campanelli M., Lousto C. O., Zlochower Y. & Merritt D., 2007, ApJ, 659, 5
- [20] Madau P., Rees M. J., Volonteri M., Haardt F. & Oh, S. P., 2004, ApJ 604, 484
- [21] Merritt D., Milosavljevic M., Favata M., Hughes S. A. & Holz D. E., 2004, Apj, 607, 9
- [22] Volonteri M., 2007, ApJ, 663, 5
- [23] White S. D. M. & Rees M. J., 1978, MNRAS, 310, 645
- [24] Peebles P. J. E., 1982, Apj, 263, 1
- [25] Press W. H. & Schechter P., 1974, ApJ, 187, 425
- [26] Lacey C. & Cole S., 1993, MNRAS, 262, 627
- [27] Sheth R. K. & Tormen G., 1999, MNARS, 308, 119
- [28] Tremaine S. et al., 2002, ApJ, 574, 740
- [29] Kazantzidis S. et al., 2005, Apj, 623, 67
- [30] Begelman M. C., Blandford R. D. & Rees M. J., 1980, Nature, 287, 307
- [31] Escala A., Larson R. B., Coppi P. S. & Mardones D., 2005, ApJ, 607, 765
- [32] Dotti M., Colpi M. & Haardt F., 2006, MNRAS, 367, 103
- [33] Flanagan E. E. & Hughes S. A., 1998, PhRvD, 57, 4535
- [34] Nelemans G., Yungelson L. R. & Portegies-Zwart S. F., 2001, A&A, 375, 890
- [35] Farmer A. J. & Phinney E. S., 2003, MNRAS, 346, 1197
- [36] Barack L. & Cutler C., 2004, PhRvD, 70l2002B
- [37] Favata M., Hughes S. A. & Holz D. E., 2004, ApJ, 607, 5
- [38] Baker J. G., Centrella J., Choi D. I., Koppitz M., van Meter J. R. & Miller M. C., 2006, ApJ, 653, 93
- [39] Heger, A., & Woosley, S. E. 2002, ApJ, 567, 532
- [40] Bullock J. S., Dekel A., Kolatt T. S., Kravtsov A. V., Klypin A. A., Porciani C. & Primack J. R., 2001, MNRAS, 321, 559
- [41] van der Bosch F. C., Abel T., Croft R. A. C., Hernquist L., White S. D. M., 2002, ApJ, 576, 21
- [42] Shlosman I., Frank J., Begelman M. C., 1989, Nature, 338, 45